

CO₂ capture using aqueous solutions of K₂CO₃+2-methylpiperazine and monoethanolamine: Specific heat capacity and heat of absorption

Young Eun Kim, Jeong Ho Choi, Soung Hee Yun, Sung Chan Nam, and Yeo Il Yoon[†]

Green Energy Process Laboratory, Climate Change Research Division, Korea Institute of Energy Research,
152 Gajeong-ro, Yuseong-gu, Daejeon 34129, Korea
(Received 25 March 2016 • accepted 28 June 2016)

Abstract—The specific heat capacity, heat of CO₂ absorption, and CO₂ absorption capacity of aqueous solutions of potassium carbonate (K₂CO₃)+2-methylpiperazine (2-MPZ) and monoethanolamine (MEA) were measured over various temperatures. An aqueous solution of K₂CO₃+2-MPZ is a promising absorbent for CO₂ capture because it has high CO₂ absorption capacity with improved absorption rate and degradation stability. Aqueous solution of MEA was used as a reference absorbent for comparison of the thermodynamic characteristics. Specific heat capacity was measured using a differential scanning calorimeter (DSC), and heat of CO₂ absorption and CO₂ absorption capacity were measured using a differential reaction calorimeter (DRC). The CO₂-loaded solutions had lower specific heat capacities than those of fresh solutions. Aqueous solutions of K₂CO₃+2-MPZ had lower specific heat capacity than those of MEA over the temperature ranges of 303–353 K. Under the typical operating conditions for the process (CO₂ loading=0.23 mol-CO₂·mol⁻¹-solute in fresh solution, T=313 K), the heat of absorption ($-\Delta H_{abs}$) of aqueous solutions of K₂CO₃+2-MPZ and MEA were approximately 49 and 75 kJ·mol-CO₂, respectively. The thermodynamic data from this study can be used to design a process for CO₂ capture.

Keywords: CO₂ Capture, Absorption, Monoethanolamine, Potassium Carbonate

INTRODUCTION

The reduction of greenhouse gases is more becoming important because of natural disasters caused by global warming. Carbon dioxide (CO₂) capture, usage and storage (CCUS) is one of the solutions needed to reduce CO₂ emissions from industrial facilities. Chemical absorption using aqueous solutions of amine is the most commonly used in the CO₂ capture process. The conventional absorption process using chemical absorbents consists of the CO₂ absorber and the stripper [1,2]. In the absorber, CO₂-containing gas is put in contact with an absorbent counter-current. When the CO₂-rich solution is heated (373–393 K), the absorbent is regenerated, and high-purity CO₂ gas is released from the top of the stripper. Therefore, the reboiler heat duty of the stripper is the major energy penalty in the process [3–5]. The heat required to regenerate the absorbent can be represented as follows [6]:

$$Q_{reg} = Q_{sens} + Q_{vap, H_2O} + Q_{abs, CO_2} \quad (1)$$

where Q_{sens} is the sensible heat required to raise the temperature of the absorbent downstream of the heat exchanger to the reboiler temperature, Q_{vap, H₂O} is the heat of evaporation required to produce stripping steam in the reboiler, and Q_{abs, CO₂} is heat of CO₂ absorption.

Good data on the heat capacity and heat of CO₂ absorption of the absorbents are required to design the absorption process. Sev-

eral researchers have measured and/or calculated heat capacities [7–13] and heats of CO₂ absorption [14–24] of aqueous solutions of amine. Among them, the researchers studied heat of CO₂ absorption of aqueous solutions of alkanolamines: primary amine, monoethanolamine (MEA) [14–19] and 2-amino-2-methyl-1-propanol (AMP) [18–20]; secondary amine, diethanolamine (DEA) [19,21]; tertiary amine, triethanolamine (TEA) [19] and methyldiethanolamine (MDEA) [19,22]. The results showed that heat of CO₂ absorption of these substances, represented by enthalpy changes ($-\Delta H_{abs}$), followed the order: TEA < MDEA < DEA < MEA. Kim and Svendsen [23] measured heats of CO₂ absorption of aqueous solutions of various amines and amine blends. Chen and Rochelle [24] calculated the heats of CO₂ absorption of concentrated aqueous solutions of piperazine derivatives. The $-\Delta H_{abs}$ values of all the piperazine (PZ) derivatives were around 70 kJ·mol⁻¹-CO₂ (cf. 7 m MEA: 81–84 kJ·mol⁻¹-CO₂) at 313 K.

CO₂ absorption process using aqueous solution of potassium carbonate (K₂CO₃) is effective at high temperatures and pressures (e.g., the Benfield process). At low temperatures, however, the performance of the aqueous solution of K₂CO₃ is limited by several factors, such as a slow CO₂ absorption rate and solid salt (potassium bicarbonate, KHCO₃) formation. Various amines have been added to aqueous solutions of K₂CO₃ to hybridize their CO₂ absorption performance. Laddha and Danckwerts [25] studied the kinetics of the reactions of aqueous solutions of K₂CO₃+MEA and K₂CO₃+DEA; the presence of electrolytes appeared to increase the rates of reaction between CO₂ and these amines. Several researchers concluded that adding certain amines to aqueous solutions of K₂CO₃ enhanced absorption rates and reduced heat of absorption at typical absorber conditions for CO₂ removal [26–29]. Cullinane

[†]To whom correspondence should be addressed.

E-mail: 21yoon@kier.re.kr

[‡]This article is dedicated to Prof. Sung Hyun Kim on the occasion of his retirement from Korea University.

Copyright by The Korean Institute of Chemical Engineers.

and Rochelle [27] measured the CO₂ absorption rates into aqueous solutions of K₂CO₃+PZ in a wetted-wall column (WWC). The CO₂ absorption rate into the aqueous solution of 20 wt% K₂CO₃+5 wt% PZ was found to be similar to that of an aqueous solution of 30 wt% MEA. The addition of PZ to the aqueous solution of K₂CO₃ increased the absorption capacity because the large quantity of bicarbonate (HCO₃⁻)/carbonate (CO₃²⁻) in the solutions served as a buffer that reduced the protonation of PZ [28,29].

K₂CO₃ forms ions such as K⁺, OH⁻, and HCO₃⁻ in the aqueous solution. In the pH range of interest for commercial operation (pH >10), and using an aqueous K₂CO₃ solution, the predominant reaction is the direct reaction between the CO₂ (aq) and the hydroxyl ion (OH⁻) as indicated in reaction of Eq. (2) [30].



The general reaction mechanism for both inorganic and organic rate-promotion-additives in the carbonate solution can be represented as following the two steps indicated by reactions in Eqs. (4) and (5) [30,31]:



The difference between the homogeneous catalysis and shuttle mechanism additives is related to the relative rate of the second step (Eq. (5)) [32]. If the promoter is a kind of primary or secondary amine, in the region near the gas-liquid interface, CO₂ reacts with promoter to form an intermediate. When the amine type promoter is used at moderate temperature, this reaction of Eq. (4) is fast enough to enhance the mass transfer rate, while the reaction of Eq. (5) is so much slower that it can only take place in the bulk of the liquid.

Aqueous solution of K₂CO₃+2-methylpiperazine (2-MPZ), is a promising absorbent-combination due to its high CO₂ absorption capacity and degradation stability, and is expected to have a low heat of absorption [33,34]. However, there is no literature presenting the specific heat capacity and heat of CO₂ absorption data for this absorbent. Therefore, we investigated the physical and thermodynamic characteristics of the aqueous solution of K₂CO₃+2-MPZ to obtain information for CO₂ capture process design.

EXPERIMENTAL

1. Materials

Absorbent concentrations of 15+5, 15+7.5, and 15+10 wt% K₂CO₃+2-MPZ were prepared using deionized water. The absorbent concentrations selected were determined based on the results of the previous study [33]. Aqueous solutions of 20-30 wt% MEA have been used in industrial processes [35]; therefore, 20, 22.5, 25, and 30 wt% aqueous solutions of MEA were prepared using deionized water for comparison. The following reagents were used as received: K₂CO₃ (Samchun Chemicals Co. Korea, anhydrous 99.5%), 2-MPZ (Acros Co., 98%), and MEA (Sigma-Aldrich Co., 99%). 30 vol% CO₂ gas mixed with 70 vol% N₂ was used to obtain the heat of CO₂ absorption in the absorbents, using a differential reaction calorimeter (DRC).

2. Experimental Procedure

The specific heat capacities of the fresh and CO₂-loaded absorbents were measured with a differential scanning calorimeter (DSC) (μ DSC3 evo model, Setaram Co.) [34]. Two closed batch cells, a reference cell and a measuring cell, were used in the specific heat capacity measurements. The measuring cell was filled with samples and put in the calorimetric block. Before measurement was started, the temperature of the furnace was kept at the initial temperature of 300.5 K for at least 10 min. The initial and final temperatures were maintained for 20 min at 300.5 K and 355.5 K, respectively, and the scanning rate was 0.2 K·min⁻¹. The CO₂-loaded samples for specific heat capacity measurements were prepared by using a semi-batch-type absorption apparatus. The configuration and experimental procedure of the semi-batch-type apparatus were similar to that previously reported except for the reactor size (diameter, height) and gas flow rate [36]. The reactor (internal volume 500 mL) was filled with 250 mL of fresh absorbent. Then, 30 vol% CO₂ was injected at a rate of 500 mL·min⁻¹ using a mass flow controller (MFC; 5850E model, Brooks Co.). Gas emitted from the reactor was sent to the gas chromatograph (GC; 7890A model, Agilent Co.) for measuring CO₂ concentration. The CO₂ loading of the absorbents was calculated by gas analysis using the GC.

The heat of CO₂ absorption of the absorbents was measured with a DRC (Setaram Co.). The experimental apparatus and procedure were described in previous publications [36,37]. The reactors (internal volume 250 mL) were each filled with 150 g of absorbent, and were stirred at 250 rpm. Next, 99.999 vol% N₂ was piped into the measuring reactor to remove impurities, and then 30 vol% CO₂ was injected into the measuring reactor at a flow rate of 150 mL·min⁻¹ by using an MFC.

RESULTS AND DISCUSSION

1. Specific Heat Capacity

Figs. 1 and 2 represent specific heat capacity (C_p) values over the temperature range from 303 to 353 K. The measurements were conducted four times for every sample in this study, and average values were used in Figs. 1 and 2.

The standard deviation (SD) of the data was calculated by fol-

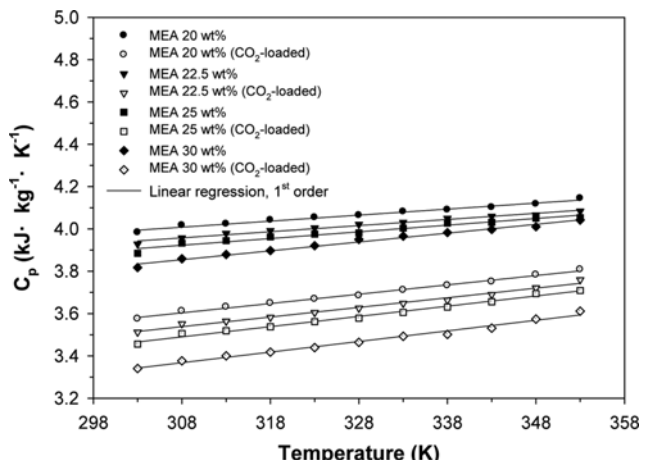


Fig. 1. Specific heat capacities of aqueous solutions of MEA.

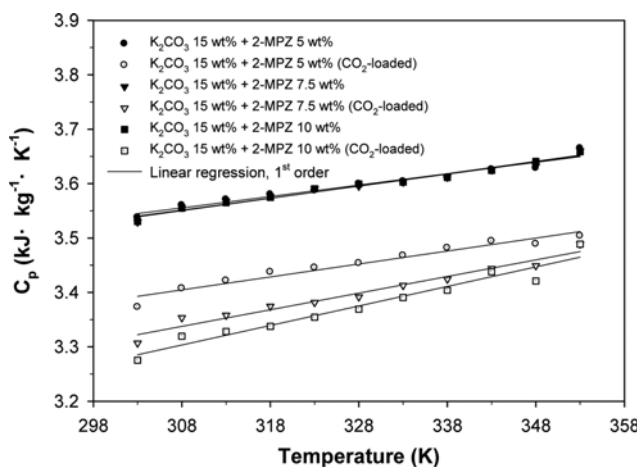


Fig. 2. Specific heat capacities of aqueous solutions of K₂CO₃+2-MPZ.

lowing equation:

$$SD = \sqrt{\frac{\sum_{i=1}^n (X_i - \bar{X})^2}{n-1}} \quad (6)$$

where X_i and \bar{X} are each value in the population and the mean of the sample, respectively, and n is the number of values in the sample. The relative standard deviation percent (%RSD) was calculated as follows:

$$\%RSD = \frac{SD}{\bar{X}} \cdot 100 \quad (7)$$

Standard uncertainty of the mean (SU) and the relative standard

uncertainty percent (%RSU) were calculated using Eqs. (8) and (9) (A-type method).

$$SU = \frac{SD}{\sqrt{n}} \quad (8)$$

$$\%RSU = \frac{SU}{\bar{X}} \cdot 100 \quad (9)$$

The %RSD of C_p value measurements of fresh MEA solutions and CO₂-loaded MEA solutions were 0.03-0.70% and 0.08-0.83%, respectively. The %RSD of the C_p value measurements of the fresh K₂CO₃+2-MPZ solutions, and CO₂-loaded K₂CO₃+2-MPZ solutions were 0.44-0.97% and 0.07-1.32%, respectively. All %RSU of the C_p values in this study were less than 0.4%.

The CO₂-loaded absorbents had lower C_p values than those of fresh absorbents. The C_p values of fresh MEA solutions decreased according to increasing concentration of MEA (20→30 wt%), whereas concentrations of 2-MPZ in the fresh K₂CO₃+2-MPZ solutions did not affect C_p values. Furthermore, K₂CO₃+2-MPZ solutions had lower C_p values than those of MEA over the temperature range 303-353 K. The CO₂-loaded absorbents had lower C_p than those of fresh absorbents. The specific heat capacity, C_p, was expressed as the unit of kJ·kg⁻¹·K⁻¹. CO₂-loaded absorbent comprises species derived from solute (K₂CO₃ and/or amine)-H₂O-CO₂ system, and fresh absorbent consists of solute and H₂O. The percentage of species in the samples was changed according to CO₂ loading. The difference affects the physical properties.

Tables 1 and 2 present the C_p values and the equation parameters of the C_p of aqueous solutions of MEA and K₂CO₃+2-MPZ. The parameters in Tables 1 and 2 were obtained from first-order linear regression presented in Figs. 1 and 2.

Table 1. Parameters for the linear regression of C_p values of aqueous solutions of MEA

Absorbent (wt%)	CO ₂ loading (mol CO ₂ /mol MEA)	a ^a	10 ⁻³ b ^a	R ²
MEA 20	Fresh solution	3.1315	2.8478	0.9839
	0.634	2.2470	4.4044	0.9940
MEA 22.5	Fresh solution	3.0666	2.8945	0.9815
	0.616	2.1374	4.5492	0.9877
MEA 25	Fresh solution	2.9523	3.1530	0.9648
	0.597	1.9983	4.8434	0.9903
MEA 30	Fresh solution	2.5661	4.1847	0.9865
	0.581	1.8252	5.0097	0.9862

^aC_p(kJ·kg⁻¹·K⁻¹)=a+b·T

Table 2. Parameters for the linear regression of C_p values of aqueous solutions of K₂CO₃+2-MPZ

Absorbent (wt%)	CO ₂ loading (mol CO ₂ /(mol K ₂ CO ₃ +mol 2-MPZ)))	a ^a	10 ⁻³ b ^a	R ²
K ₂ CO ₃ 15+2-MPZ 5	Fresh solution	2.9096	2.0964	0.9580
	0.898	2.6704	2.3836	0.9518
K ₂ CO ₃ 15+2-MPZ 7.5	Fresh solution	2.8725	2.2038	0.9683
	0.902	2.3969	3.0542	0.9645
K ₂ CO ₃ 15+2-MPZ 10	Fresh solution	2.8510	2.2703	0.9791
	0.860	2.1992	3.5851	0.9510

^aC_p(kJ·kg⁻¹·K⁻¹)=a+b·T

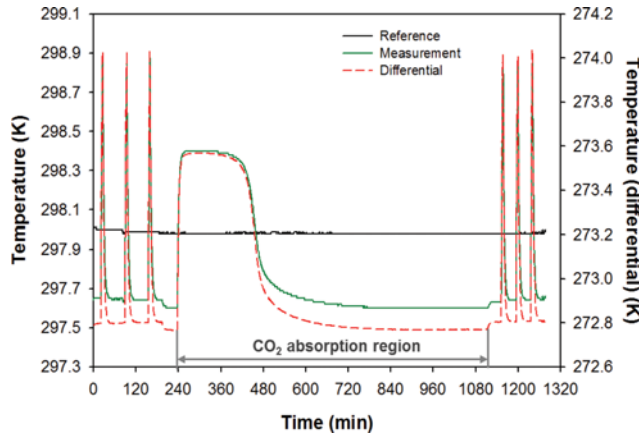


Fig. 3. DRC curves of aqueous solutions of 30 wt% MEA during CO_2 absorption at 298 K.

2. Heat of Absorption and CO_2 Loading Capacity

The differential temperature (T_{diff}) curve between the reference cell and the measuring cell over time was obtained from DRC experiments. The T_{diff} curve was used to calculate the heat of CO_2 absorption represented by enthalpy changes during CO_2 absorption ($-\Delta H_{\text{abs}}$). Fig. 3 shows the temperature curves from DRC experiments for the aqueous 30 wt% MEA solution at 298 K.

The experimental temperature ranges of DRC experiments (298, 303, and 313 K) were absorption conditions used in conventional absorption processes. The heat of absorption and CO_2 loading capacity of aqueous solutions of MEA and $\text{K}_2\text{CO}_3+2\text{-MPZ}$ are shown in Fig. 4, and the individual values are presented in Tables 3-8. The CO_2 absorption capacity can be represented as CO_2 loading ($\text{mol}\text{-CO}_2\cdot\text{mol}^{-1}\text{-solute}$ in fresh solution). The heat of absorption was calculated at the CO_2 loadings of 1/4, 1/2, and 3/4 of the reaction endpoint, and at CO_2 loading ($\text{mol}\text{-CO}_2\cdot\text{mol}^{-1}\text{-solute}$ in fresh solution)=0.23 for comparison. Generally, in the typical MEA process, CO_2 loading of the CO_2 -lean solution is maintained at 0.15-0.30 [38-40]. At CO_2 loading=0.23 and $T=313\text{ K}$, the heat of absorption of the $\text{K}_2\text{CO}_3+2\text{-MPZ}$ and MEA solutions was approximately 49 and 75 $\text{kJ}\cdot\text{mol}^{-1}\text{-CO}_2$, respectively. Increase in the amine concentration did not significantly affect the heat of absorption within the range of this study. Furthermore, temperature dependence of the heat of absorption was weak for MEA and $\text{K}_2\text{CO}_3+2\text{-MPZ}$ absorbents at 298-313 K. A similar result of weak temperature dependence on heat of absorption was also shown in the literature [41].

The moles of CO_2 ($\text{mol}\text{-CO}_2$) in the CO_2 -saturated MEA solutions was higher than that in the $\text{K}_2\text{CO}_3+2\text{-MPZ}$; however, the CO_2 loading ($\text{mol}\text{-CO}_2\cdot\text{mol}^{-1}\text{-solute}$ in fresh solution) of aqueous solutions of MEA was lower than that of $\text{K}_2\text{CO}_3+2\text{-MPZ}$. The CO_2 -saturated solution contains maximum amount of CO_2 that absorbent can absorb CO_2 at the specific condition. The heat of absorption of CO_2 in the aqueous solutions of $\text{K}_2\text{CO}_3+2\text{-MPZ}$ was lower than that of aqueous solutions of MEA. These results can be explained by differences in the reaction mechanisms presented below. Theoretically, one mole of MEA can react with 0.5 mole of CO_2 . In the aqueous MEA solution, MEA (RNH_2) reacts with CO_2 to form an intermediate (zwitterion, $\text{RNH}_2^+\text{COO}^-$), and the zwitter-

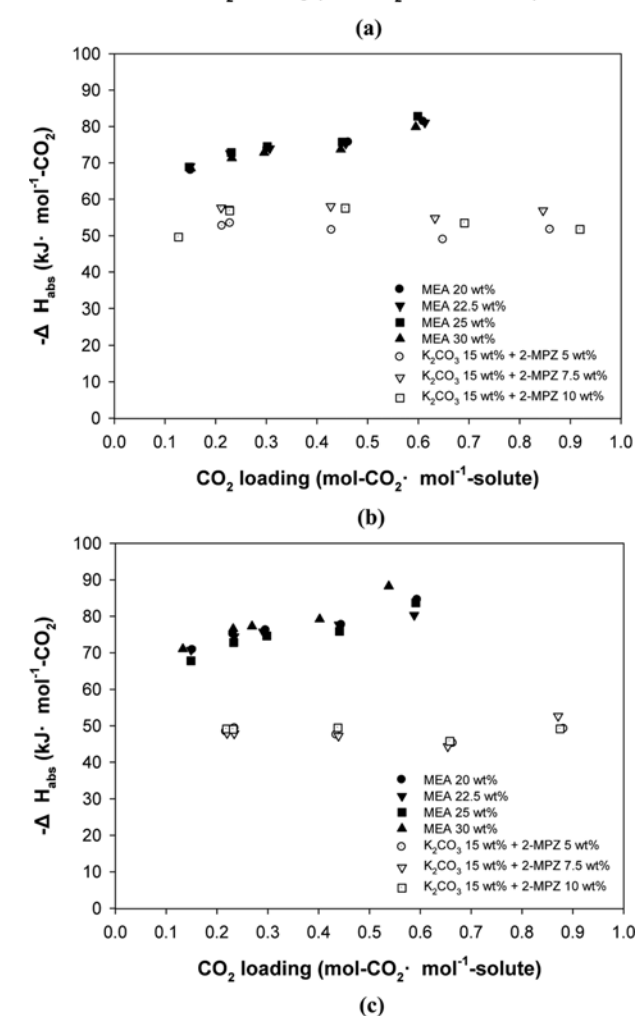
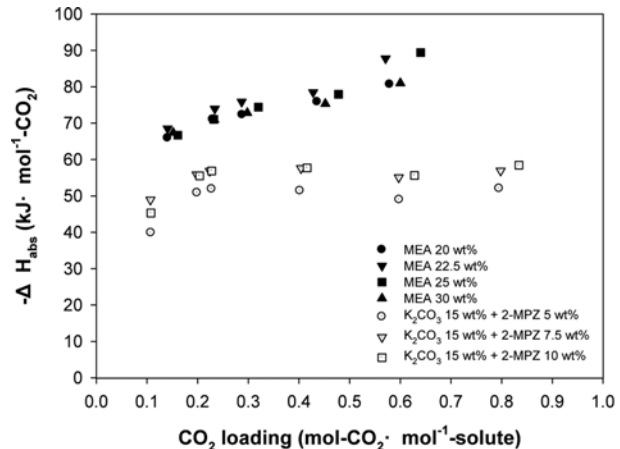


Fig. 4. Heats of CO_2 absorption of aqueous solutions of $\text{K}_2\text{CO}_3+2\text{-MPZ}$ and MEA: (a) 298 K; (b) 303 K; (c) 313 K.

ion reacts with base (RNH_2 , OH^- , H_2O) in the solution [32,42,43]. More specifically, the zwitterion ($\text{RNH}_2^+\text{COO}^-$) primarily reacts with MEA (RNH_2) and forms MEA carbamate (RNHCOO^-) and protonated MEA (RNH_3^+). In the aqueous 2-MPZ solution, 2-MPZ reacts with CO_2 to form 2-MPZ carbamate (2-MPZCOO^-) and 2-MPZ bicarbamate (2-MPZ(COO)_2^-); however, the amount

Table 3. Heats of CO₂ absorption in aqueous solutions of MEA at 298 K

Absorbent (wt%)	CO ₂ loading		-ΔH _{abs} (kJ/mol CO ₂)	-Q (kJ)
	(mol CO ₂)	(mol CO ₂ /mol MEA)		
MEA 20	0.069	0.141	65.914	1.498
	0.113	0.230	71.037	1.614
	0.142	0.288	72.304	1.643
	0.214	0.436	75.860	1.724
	0.285	0.579	80.647	1.833
MEA 22.5	0.078	0.141	68.486	1.557
	0.129	0.234	73.954	1.681
	0.158	0.287	75.847	1.724
	0.236	0.428	78.478	1.784
	0.315	0.571	87.753	1.994
MEA 25	0.099	0.161	66.680	1.515
	0.143	0.232	71.035	1.614
	0.197	0.320	74.381	1.690
	0.294	0.478	77.943	1.771
	0.393	0.640	89.413	2.032
MEA 30	0.112	0.152	67.387	1.532
	0.172	0.233	70.938	1.612
	0.219	0.298	72.835	1.655
	0.333	0.452	75.319	1.712
	0.442	0.600	80.980	1.840

Table 4. Heats of CO₂ absorption in aqueous solutions of MEA at 303 K

Absorbent (wt%)	CO ₂ loading		-ΔH _{abs} (kJ/mol CO ₂)	-Q (kJ)
	(mol CO ₂)	(mol CO ₂ /mol MEA)		
MEA 20	0.074	0.151	67.962	1.545
	0.113	0.231	72.597	1.650
	0.149	0.302	73.924	1.680
	0.227	0.462	75.667	1.720
	0.300	0.610	81.371	1.849
MEA 22.5	0.083	0.150	69.084	1.570
	0.126	0.229	72.666	1.652
	0.170	0.307	73.970	1.681
	0.253	0.457	75.278	1.711
	0.339	0.613	81.035	1.842
MEA 25	0.091	0.148	68.863	1.565
	0.142	0.231	72.857	1.656
	0.185	0.302	74.510	1.693
	0.276	0.450	75.716	1.721
	0.368	0.599	82.784	1.881
MEA 30	0.111	0.151	68.520	1.557
	0.171	0.232	71.296	1.620
	0.218	0.296	72.847	1.656
	0.329	0.447	73.717	1.675
	0.438	0.595	79.884	1.816

of bicarbamate could be small due to hydrolysis of the carbamate adjacent to methyl groups causing steric hindrance [34]. The CO₂

absorption mechanism of the aqueous solution of K₂CO₃+2-MPZ complies with the shuttle mechanism mentioned in the Introduc-

Table 5. Heats of CO₂ absorption in aqueous solutions of MEA at 313 K

Absorbent (wt%)	CO ₂ loading		−ΔH _{abs} (kJ/mol CO ₂)	−Q (kJ)
	(mol CO ₂)	(mol CO ₂ /mol MEA)		
MEA 20	0.075	0.152	70.809	1.609
	0.114	0.232	75.071	1.706
	0.145	0.296	76.204	1.732
	0.219	0.445	77.670	1.765
	0.292	0.594	84.516	1.921
MEA 22.5	0.082	0.149	70.803	1.609
	0.129	0.234	74.477	1.693
	0.161	0.291	75.780	1.722
	0.243	0.440	77.689	1.766
	0.325	0.588	80.351	1.826
MEA 25	0.092	0.149	67.823	1.541
	0.143	0.233	72.847	1.656
	0.183	0.298	74.626	1.696
	0.271	0.441	75.884	1.725
	0.363	0.591	83.720	1.903
MEA 30	0.098	0.133	71.051	1.615
	0.171	0.232	76.567	1.740
	0.198	0.269	77.275	1.756
	0.296	0.402	79.222	1.801
	0.397	0.538	88.242	2.006

Table 6. Heats of CO₂ absorption in aqueous solutions of K₂CO₃+2-MPZ at 298 K

Absorbent (wt%)	CO ₂ loading		−ΔH _{abs} (kJ/mol CO ₂)	−Q (kJ)
	(mol CO ₂)	(mol CO ₂ /(mol K ₂ CO ₃ +mol 2-MPZ))		
K ₂ CO ₃ 15+2-MPZ 5	0.026	0.108	39.875	0.906
	0.047	0.199	50.859	1.156
	0.054	0.228	51.888	1.179
	0.096	0.402	51.423	1.169
	0.142	0.598	48.943	1.112
	0.189	0.795	52.025	1.182
K ₂ CO ₃ 15+2-MPZ 7.5	0.029	0.107	48.928	1.112
	0.055	0.198	55.864	1.270
	0.062	0.224	56.867	1.292
	0.111	0.404	57.596	1.309
	0.164	0.597	55.087	1.252
	0.220	0.798	56.921	1.294
K ₂ CO ₃ 15+2-MPZ 10	0.034	0.108	45.285	1.029
	0.064	0.204	55.506	1.262
	0.071	0.228	56.868	1.292
	0.130	0.416	57.713	1.312
	0.196	0.628	55.626	1.264
	0.261	0.834	58.429	1.328

tion. A large amount of bicarbonate/carbonate is formed in the aqueous solutions of K₂CO₃+2-MPZ, but the CO₂ is relatively easier to decompose from the bicarbonate/carbonate by heating, than from carbamate.

CONCLUSIONS

The physical properties and CO₂ absorption characteristics of aqueous solutions of K₂CO₃+2-MPZ were investigated. The spe-

Table 7. Heats of CO₂ absorption in aqueous solutions of K₂CO₃+2-MPZ at 303 K

Absorbent (wt%)	CO ₂ loading		-ΔH _{abs}		-Q
	(mol CO ₂)	(mol CO ₂ /(mol K ₂ CO ₃ +mol 2-MPZ))	(kJ/mol CO ₂)	(kJ/g CO ₂)	(kJ)
K ₂ CO ₃ 15+2-MPZ 5	0.051	0.213	52.649	1.197	2.685
	0.055	0.229	53.398	1.214	2.937
	0.102	0.429	51.526	1.171	5.256
	0.154	0.649	48.911	1.112	7.532
	0.204	0.860	51.640	1.174	10.535
K ₂ CO ₃ 15+2-MPZ 7.5	0.058	0.211	57.672	1.311	3.345
	0.062	0.226	57.350	1.303	3.556
	0.117	0.427	58.065	1.320	6.794
	0.174	0.633	54.811	1.246	9.537
	0.233	0.846	56.915	1.294	13.261
K ₂ CO ₃ 15+2-MPZ 10	0.040	0.127	49.606	1.127	1.984
	0.071	0.228	56.816	1.291	4.034
	0.143	0.456	57.524	1.307	8.256
	0.216	0.691	53.464	1.215	11.548
	0.287	0.919	51.729	1.176	14.846

Table 8. Heats of CO₂ absorption in aqueous solutions of K₂CO₃+2-MPZ at 313 K

Absorbent (wt%)	CO ₂ loading		-ΔH _{abs}		-Q
	(mol CO ₂)	(mol CO ₂ /(mol K ₂ CO ₃ +mol 2-MPZ))	(kJ/mol CO ₂)	(kJ/g CO ₂)	(kJ)
K ₂ CO ₃ 15+2-MPZ 5	0.052	0.218	48.354	1.099	2.514
	0.056	0.235	49.334	1.121	2.763
	0.103	0.435	47.485	1.079	4.891
	0.158	0.664	45.199	1.027	7.142
	0.210	0.882	49.158	1.117	10.323
K ₂ CO ₃ 15+2-MPZ 7.5	0.060	0.220	47.981	1.090	2.879
	0.064	0.234	47.896	1.089	3.065
	0.121	0.439	47.222	1.073	5.714
	0.180	0.654	44.343	1.008	7.982
	0.240	0.871	52.647	1.167	12.635
K ₂ CO ₃ 15+2-MPZ 10	0.068	0.219	49.123	1.116	3.340
	0.072	0.232	49.034	1.114	3.530
	0.137	0.438	49.443	1.124	6.774
	0.206	0.658	45.756	1.040	9.426
	0.274	0.875	49.150	1.117	13.467

cific heat capacity of fresh and CO₂-loaded K₂CO₃+2-MPZ solutions was measured in the temperature range 300 to 353 K, using DSC. Heat of absorption and CO₂ loading capacity of aqueous solutions of K₂CO₃+2-MPZ were measured at 303 and 313 K, which are temperatures typically used in conventional CO₂ absorption processes. CO₂-loaded solutions of K₂CO₃+2-MPZ had lower C_p values than those of fresh absorbents. Concentrations of 2-MPZ (5, 7.5, 10 wt%) in aqueous solutions of K₂CO₃+2-MPZ did not affect C_p values; however, C_p values of the absorbents decreased after CO₂ absorption. The C_p values of fresh aqueous solutions of 15 wt% K₂CO₃+10 wt% 2-MPZ were lower than those of aqueous solutions of 30 wt% MEA; however, C_p values of CO₂-saturated solutions were similar. Temperature and amine concentration did not significantly

affect the heat of absorption within the range of this study; however, the heat of absorption was changed according to CO₂ loading. Aqueous solutions of K₂CO₃+2-MPZ have the advantages of lower heat of absorption and higher CO₂ loading capacity, compared to MEA. Although the heat of absorption is directly related to regeneration energy of absorbent, other important factors such as CO₂ loading capacity, absorption rate, and physical properties are also thoroughly considered for selection of absorbent.

ACKNOWLEDGEMENTS

This work was supported by the Energy Demand Management Technology Program of the Korea Institute of Energy Technology

Evaluation and Planning (KETEP), granted financial resource from the Ministry of Trade, Industry and Energy, Republic of Korea (No. 20152010201940).

REFERENCES

1. F. Barzaghi, F. Mani and M. Peruzzini, *Energy Environ. Sci.*, **3**, 772 (2010).
2. M. Ahmadi, V.G. Gomes and K. Ngian, *Sep. Purif. Technol.*, **63**, 107 (2008).
3. J. Oexmann, A. Kather, S. Linnenberg and U. Liebenthal, *Greenhouse Gas Sci. Technol.*, **2**, 80 (2012).
4. M. Wang, A. Lawal, P. Stephenson, J. Sidders, C. Ramshaw and H. Yeung, *Chem. Eng. Res. Des.*, **89**, 1609 (2011).
5. T. Yokoyama, *Sep. Purif. Technol.*, **94**, 97 (2012).
6. J. Oexmann and A. Kather, *Int. J. Greenhouse Gas Control*, **4**, 36 (2010).
7. R. H. Weiland, J.C. Dingman and D. B. Cronin, *J. Chem. Eng. Data*, **42**, 1004 (1997).
8. L.-F. Chiu, H.-F. Liu and M.-H. Li, *J. Chem. Eng. Data*, **44**, 631 (1999).
9. L.-F. Chiu and M.-H. Li, *J. Chem. Eng. Data*, **44**, 1396 (1999).
10. Y.-J. Chen and M.-H. Li, *J. Chem. Eng. Data*, **46**, 102 (2001).
11. Y.-J. Chen, T.-W. Shih and M.-H. Li, *J. Chem. Eng. Data*, **46**, 51 (2001).
12. F. Harris, K.D. Kurnia, M. I. A. Mutualib and T. Murugesan, *J. Chem. Eng. Data*, **55**, 547 (2010).
13. H.-J. Song, M.-G. Lee, H. Kim, A. Gaur and J.-W. Park, *J. Chem. Eng. Data*, **56**, 1371 (2011).
14. I. Kim and H. F. Svendsen, *Ind. Eng. Chem. Res.*, **46**, 5803 (2007).
15. N. McCann, M. Maeder and M. Attalla, *Ind. Eng. Chem. Res.*, **47**, 2002 (2008).
16. F. Qin, S. Wang, I. Kim, H. F. Svendsen and C. Chen, *Int. J. Greenhouse Gas Control*, **5**, 405 (2011).
17. H. Arcis, K. Ballerat-Busserolles, L. Rodier and J.-Y. Coxam, *J. Chem. Eng. Data*, **56**, 3351 (2011).
18. T. Filburn, J.J. Helble and R. A. Weiss, *Ind. Eng. Chem. Res.*, **44**, 1542 (2005).
19. I. Kim, K. A. Hoff, E. T. Hessen, T. Haug-Warberg and H. F. Svendsen, *Chem. Eng. Sci.*, **64**, 2027 (2009).
20. H. Arcis, L. Rodier and J.-Y. Coxam, *J. Chem. Thermodyn.*, **39**, 878 (2007).
21. H. Arcis, K. Ballerat-Busserolles, L. Rodier and J.-Y. Coxam, *J. Chem. Eng. Data*, **57**, 840 (2012).
22. H. Arcis, L. Rodier, K. Ballerat-Busserolles and J.-Y. Coxam, *J. Chem. Thermodyn.*, **41**, 783 (2009).
23. I. Kim and H. F. Svendsen, *Int. J. Greenhouse Gas Control*, **5**, 390 (2011).
24. X. Chen and G. T. Rochelle, *Chem. Eng. Res. Des.*, **87**, 1693 (2011).
25. S. S. Laddha and P. V. Danckwerts, *Chem. Eng. Sci.*, **37**, 665 (1982).
26. R. Ramazani, S. Mazinani, A. Hafizi, A. Jahanmiri, Van der Bruggen and S. Darvishmanesh, *Sep. Sci. Technol.*, **51**, 327 (2016).
27. J. T. Cullinane and G. T. Rochelle, *Chem. Eng. Sci.*, **59**, 3619 (2004).
28. J. T. Cullinane, Ph.D. Dissertation, University of Texas (2005).
29. J. T. Cullinane and G. T. Rochelle, *Fluid Phase Equilib.*, **227**, 197 (2005).
30. A. L. Kohl and R. B. Nielsen, *Gas Purification*; 5th Ed., Gulf Publishing Company, Huston (1997).
31. X. Chen and G. T. Rochelle, *Ing. Eng. Chem. Res.*, **52**, 4229 (2013).
32. G. Astarita, D. W. Savage and J. M. Longo, *Chem. Eng. Sci.*, **36**, 581 (1981).
33. Y. E. Kim, J. H. Choi, S. C. Nam and Y. I. Yoon, *J. Ind. Eng. Chem.*, **18**, 105 (2012).
34. Y. E. Kim, S. H. Yun, J. H. Choi, S. C. Nam, S. Y. Park, S. K. Jeong and Y. I. Yoon, *Energy Fuels*, **29**, 2582 (2015).
35. M. Wang, A. Lawal, P. Stephenson, J. Sidders, C. Ramshaw and H. Yeung, *Chem. Eng. Res. Des.*, **89**, 1609 (2011).
36. Y. E. Kim, J. A. Lim, S. K. Jeong, Y. I. Yoon, S. T. Bae and S. C. Nam, *Bull. Korean Chem. Soc.*, **34**, 783 (2013).
37. J.-A. Lim, D. H. Kim, Y. Yoon, S. K. Jeong, K. T. Park and S. C. Nam, *Energy Fuels*, **26**, 3910 (2012).
38. A. B. Rao and E. S. Rubin, *Environ. Sci. Technol.*, **36**, 4467 (2002).
39. R. Sakawattanapong, A. Aroonwilas and A. Veawab, *Ind. Eng. Chem. Res.*, **44**, 4465 (2005).
40. R. Idem, M. Wilson, P. Tontiwachwuthikul, A. Chakma, A. Veawab, A. Aroonwilas and D. Gelowitz, *Ind. Eng. Chem. Res.*, **45**, 2414 (2006).
41. H. Svensson, C. Hultenberg, H. T. Karlsson, *Int. J. Greenhouse Gas Control*, **17**, 89 (2013).
42. G. F. Versteeg and W. P. M. van Swaaij, *Chem. Eng. Sci.*, **43**, 573 (1988).
43. R. J. Littel, G. F. Versteeg and W. P. M. van Swaaij, *Chem. Eng. Sci.*, **47**, 2027 (1992).